Full-Wave Modeling of Electric Coupling Probes in Comb-Line Resonators and Filters

Chi Wang, *Senior Member, IEEE,* and Kawthar A. Zaki, *Fellow, IEEE*

***Abstract*—An electric coupling probe in comb-line resonators and filters is rigorously modeled by full-wave mode matching method. The coupling structure is considered as a cascaded network of the resonator and strip-line discontinuities and is solved by cascading the generalized scattering matrices of all the discontinuities. As a result, the electric probe couplings of both rectangular and cylindrical combine resonators and filters can be accurately determined. The validation and accuracy of the method are verified by comparing the numerical results with the measured data and are shown to be in good agreement.**

***Index Terms*—Cascaded network, coupling, discontinuity, probe, resonator, ridge waveguide, scattering matrix, strip-line.**

I. Introduction

WIRELESS communications have undergone a revolution since the 1980s. The demand for ubiquitous communications has led to the development of new wireless systems like personal communication systems, wireless local-area networks and cellular systems. On the other hand, tremendous growth in wireless communications has greatly crowded the frequency spectrum, which translates into a higher likelihood of users' interfering with one another. To prevent the interference among channels, high-selectivity sharp rejection filters are required for both transmitter and receiver applications. Coaxial and comb-line filters [1], [4] with transmission zeros [2], [3] satisfying such requirements are frequently requested by the systems [10].

An electric probe is commonly used in the comb-line resonator filters to achieve the nonadjacent electric coupling for obtaining the transmission zero at the lower side or both sides of the stop band. Repeated machining and experimental adjustments usually determine the physical dimension of the coupling probe. Although pure numerical methods, such as finite-element method, can compute the coupling coefficient of the probe, the accuracy of the result depends on the computation time and memory usage. An efficient numerical technique is needed to determine the probe dimension in the comb-line filter design.

In this paper, rigorous mode matching method, one of the most efficient numerical methods, has been applied for modeling of the electric probe coupling structure in comb-line resonator filters for both rectangular and cylindrical resonator inner conductors. The rectangular inner conductor of the resonator is modeled as a piece of ridge waveguide, while the generalized scattering matrix of the cylindrical inner conductor resonator can be obtained using the modeling method described in [10] or by stair-step approximation of the ridge waveguides. The coupling structure is considered as a cascaded network of the resonator and strip-line discontinuities and is solved by cascading the generalized scattering matrices of all the discontinuities. As a result, the electric coupling of the probe can be accurately determined. The computed results are compared with both measurement and the results by finite-element method, and are shown to be in good agreement.

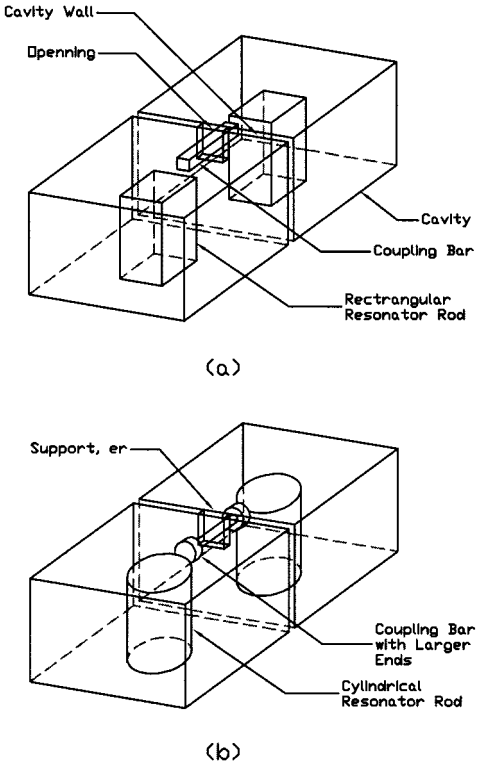

Fig. 1. Configuration of an electric coupling probe between two comb-line resonator cavities. (a) Rectangular inner conductor resonator with rectangular probe. (b) Cylindrical inner conductor comb-line resonator having cylindrical probe with larger diameter ends.

II. Configuration and Theory

Fig. 1 shows the configuration of the probe coupling resonator structure under consideration. The cross section of the resonator's inner conductor can be rectangular or cylindrical in shape, while the coupling bar or probe sits in between the two resonators through a smaller aperture in the common resonator wall. In the analysis, the rectangular inner conductor is

Manuscript received February 29, 2000; revised August 23, 2000.

C. Wang is with Radio Frequency Systems Inc., Marlboro, NJ 07746 USA.

K. A. Zaki is with the Department of Electrical Engineering, University of Maryland, College Park, MD 20742 USA.

Publisher Item Identifier S 0018-9480(00)10774-4.

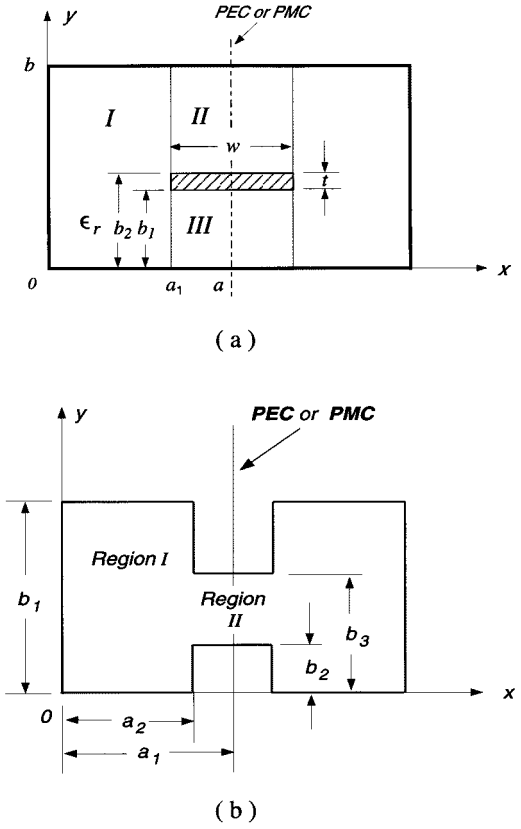

Fig. 2. (a) Cross section of a shielded strip-line. (b) Configuration of a double ridge waveguide.

considered as a piece of ridge waveguide, and the coupling bar is modeled as a strip-line within a closed enclosure. The coupling structure is symmetrical to two comb-line resonators and both sides of the coupling probe. By putting a perfect electric conductor (PEC) wall or a perfect magnetic conductor (PMC) wall at the symmetrical plane, only half of the structure needs to be considered.

A. Modeling of Strip-Line and Ridge Waveguides

The eigenmodes of the shielded strip-line and ridge waveguide are first obtained by mode matching method. Fig. 2 shows the configuration of the shielded strip-line and double ridge waveguide. The strip-line and ridge waveguide's cross sections are divided into several regions in accordance with their spatial discontinuity boundaries to be able to be modeled by mode matching method. TEM (with zero cutoff frequency), TE, and TM modes exist in the shielded strip-line, while only pure TE and TM modes exist in the ridge waveguide [6], [9].

A shielded strip-line is divided into region I, region II, and region III, as shown in Fig. 2(a). The fields of the eigenmodes are expanded by a potential function in each region for TEM mode, which satisfies the Laplace equation (7), and by normal electric or magnetic fields in each region for TE and TM mode, which satisfy the wave equations (12) and (16), respectively.

Considering only the PMC boundary condition at the symmetrical plane for TEM mode, the potential function in each region can be expressed as follows.

Region I

$$\phi = \sum_{i=1}^{n_1} A_i^{\phi} \sin(k_{y1i}^{\phi} y) \frac{sh(k_{y1i}^{\phi} x)}{sh(k_{y1i}^{\phi} a_1)}, \tag{1}$$

$$k_{y1i}^{\phi} = \frac{(i-1)\pi}{b}; \quad i = 1, 2, 3, \ldots, n_1. \tag{2}$$

Region II

$$\phi = \frac{\phi_o}{b - b_2}(b - y) + \sum_{i=1}^{n_2} B_i^{\phi} \sin(k_{y2i}^{\phi} y) \frac{ch(k_{y2i}^{\phi}(x-a))}{ch(k_{y2i}^{\phi}(a_1 - a))}, \tag{3}$$

$$k_{y2i}^{\phi} = \frac{(i-1)\pi}{b - b_2}; \quad i = 1, 2, 3, \ldots, n_2. \tag{4}$$

Region III

$$\phi = \frac{\phi_o}{b_1} y + \sum_{i=1}^{n_3} C_i^{\phi} \sin(k_{y3i}^{\phi} y) \frac{ch(k_{y3i}^{\phi}(x-a))}{ch(k_{y3i}^{\phi}(a_1 - a))}, \tag{5}$$

$$k_{y3i}^{\phi} = \frac{(i-1)\pi}{b_1}; \quad i = 1, 2, 3, \ldots, n_3. \tag{6}$$

The static potential function (x, y) satisfies the Laplace equation

$$\begin{aligned} \frac{\partial^2 \phi}{\partial x^2} + \frac{\partial^2 \phi}{\partial y^2} &= 0 \\ \phi(x,y)|_{\text{at strip-line}} &= \phi_o, \\ \phi(x,y)|_{\text{at enclosure}} &= 0. \end{aligned} \tag{7}$$

The transverse fields of the TEM mode can be obtained in terms of the potential function as

$$E_x = -\frac{\partial \phi(x,y)}{\partial x}, \quad E_y = -\frac{\partial \phi(x,y)}{\partial y} \tag{8}$$

$$H_x = +\sqrt{\frac{\epsilon}{\mu}} \frac{\partial \phi(x,y)}{\partial y}, \quad H_y = -\sqrt{\frac{\epsilon}{\mu}} \frac{\partial \phi(x,y)}{\partial x}. \tag{9}$$

Matching the tangential electromagnetic fields at the boundary of regions I, II, and III, a characteristic matrix for the TEM mode's field coefficients of the shielded strip-line can be obtained. Solving the matrix, all the field coefficients of the TEM mode can then be obtained.

Similarly, the longitudinal electric or magnetic field expressions of the TE and TM modes of the shielded strip-line and ridge waveguide can be obtained. The transverse fields of the TE and TM modes can be obtained in terms of the longitudinal components H_z for TE mode and E_z for TM modes as follows.

TE mode

$$H_x^h = -\frac{\gamma^h}{k_c^{2h}} \frac{\partial H_z^h}{\partial x}, \quad H_y^h = -\frac{\gamma^h}{k_c^{2h}} \frac{\partial H_z^h}{\partial y} \tag{10}$$

$$E_x^h = -\frac{j\omega\mu}{k_c^{2h}} \frac{\partial H_z^h}{\partial y}, \quad E_y^h = \frac{j\omega\mu}{k_c^{2h}} \frac{\partial H_z^h}{\partial x} \tag{11}$$

with

$$\nabla_t^2 H_z^h + k_c^{2h} H_z^h = 0 \tag{12}$$

$$k_c^{2h} = \gamma^{2h} + \omega^2 \mu\epsilon. \tag{13}$$

TM mode

$$H_x^e = \frac{j\omega\epsilon}{k_c^{2e}} \frac{\partial E_z^e}{\partial y}, \quad H_y^e = -\frac{j\omega\epsilon}{k_c^{2e}} \frac{\partial E_z^e}{\partial x} \tag{14}$$

$$E_x^e = -\frac{\gamma^e}{k_c^{2e}} \frac{\partial E_z^e}{\partial x}, \quad E_y^e = -\frac{\gamma^e}{k_c^{2e}} \frac{\partial E_z^e}{\partial y} \tag{15}$$

with

$$\nabla_t^2 E_z^e + k_c^{2e} E_z^e = 0, \tag{16}$$

$$k_c^{2e} = \gamma^{2e} + \omega^2 \mu\epsilon. \tag{17}$$

For TE and TM modes, both PMC and PEC boundary conditions at the symmetrical plane need to be considered in order to obtain the complete set of eigenmodes. Forcing the tangential electric and magnetic field to be continuous at boundaries, a characteristic equation for the cutoff frequency of the eigenmodes can be obtained. The cutoff frequency and field coefficients of the eigenmodes can then be obtained by searching for the zero determinant and solving the characteristic equation.

B. Strip-Line and Ridge Waveguide Discontinuities

Several kinds of discontinuities exist in the probe coupling structure between two comb-line resonators. The ridge to empty waveguide discontinuity is used to obtain the generalized scattering matrix of the comb-line resonator inner conductor section. The generalized scattering matrix of the coupling probe and conducting wall between resonators is divided into several shielded strip-line to strip-line discontinuities and strip-line to empty waveguide discontinuities. These discontinuities need to be solved to compute the probe coupling between comb-line resonators.

Fig. 3 shows the configurations of strip-line to strip-line and empty waveguide to strip-line discontinuities used for modeling of the coupling structure. Both the inner conductor and the enclosure of the two shielded strip-lines can have different cross-sections, but it requires that the strip-line with small cross section of the inner conductor have larger enclosure. The empty waveguide's cross-section should be larger than or equal to the enclosure of the shielded strip-line.

A full-wave mode-matching technique is used to obtain the generalized scattering matrices of the shielded strip-line discontinuities. The fields in the strip-line and waveguide are expressed as the superposition of the incident and reflected waves of all the eigenmodes.

The existence of TEM, TE, and TM modes in each shielded strip-line requires the following kinds of inner products between these modes:

TEM with TEM,	TE with TEM,	TM with TEM
TEM with TE,	TE with TE,	TM with TE
TEM with TM,	TE with TM,	TM with TM.

Because of the complexity of the structure, each element of the inner product matrix of the discontinuity problem involves five integrations in different regions as

$$\begin{aligned}\langle \vec{e}_t, \vec{h}_t \rangle = &\langle \vec{e}_t, \vec{h}_t \rangle_{S_{I,I}} + \langle \vec{e}_t, \vec{h}_t \rangle_{S_{I,II}} \\ &+ \langle \vec{e}_t, \vec{h}_t \rangle_{S_{I,III}} + \langle \vec{e}_t, \vec{h}_t \rangle_{S_{II,II}} \\ &+ \langle \vec{e}_t, \vec{h}_t \rangle_{S_{III,III}}\end{aligned} \tag{18}$$

where $S_{I,I} \in I_a \cup I_b, S_{II,II} \in II_a \cup II_b, S_{I,II} \in I_a \cup II_b, S_{III,III} \in III_a \cup III_b, S_{I,III} \in I_a \cup III_b$.

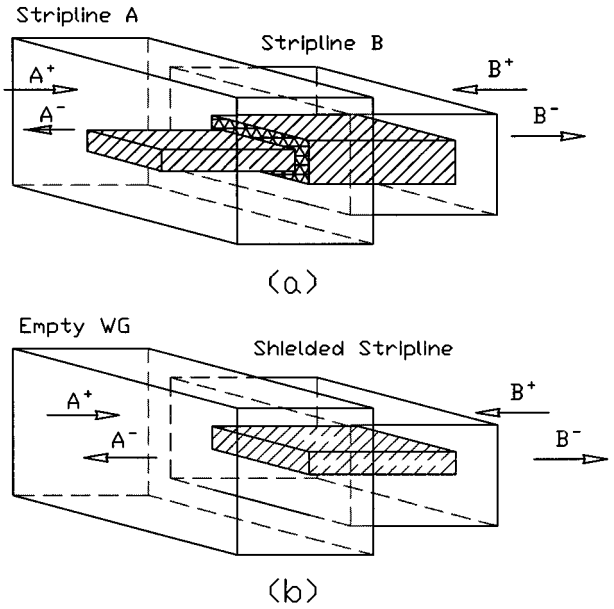

Fig. 3. (a) Configuration of a strip-line to strip-line discontinuity. (b) Configuration of empty waveguide to strip-line discontinuity.

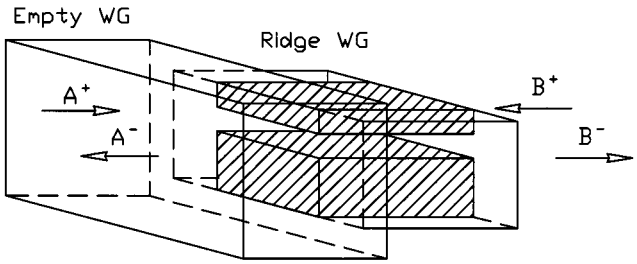

Fig. 4. A: Configuration of a ridge waveguide to ridge waveguide discontinuity. B: Configuration of empty waveguide to ridge waveguide discontinuity.

By applying boundary conditions at the interface of the discontinuity and taking proper inner product, the generalized scattering matrices of the strip-line to strip-line discontinuity can be solved.

The configuration of the generalized double ridge waveguide to empty waveguide discontinuity under consideration is shown in Fig. 4. It is required that the cross-section of the empty waveguide be larger than or equal to that of the ridge waveguide. Procedures similar to strip-line to strip-line discontinuity can be applied to obtain the generalized scattering matrices of the strip-line to empty waveguide and ridge waveguide to empty waveguide discontinuities [11].

C. Efficiency Improvement

For the homogeneous structures, all the integrations in the inner products are frequency independent, and only the attenuation constant γ and frequency f are the frequency-dependent part. By separating the inner product of the discontinuity into the product of frequency-dependent and frequency-independent parts, the inner product of the discontinuities needs to be computed only once for all frequency computations

$$\langle \vec{e}_t, \vec{h}_t \rangle = \mathcal{F}(f) \cdot \Re(x, y) \tag{19}$$

where $\mathcal{F}(f)$ is the frequency-dependent part and $\Re(x,y)$ is the geometry-dependent part inner products.

By inspecting the definition of the inner product, the frequency-dependent part of the inner product $\mathcal{F}(f)$ can be defined as

$$\begin{array}{ll} \text{TEM, TE with TEM, TE:} & \mathcal{F}(f)=\gamma_a \\ \text{TEM, TE with TM:} & \mathcal{F}(f)=f^2 \\ \text{TM with TEM, TE:} & \mathcal{F}(f)=\gamma_a\gamma_b \\ \text{TM with TM:} & \mathcal{F}(f)=f^2\gamma_b. \end{array} \tag{20}$$

With the frequency-dependent part of the inner product $\mathcal{F}(f)$, the frequency-independent part of the inner product $\Re(x,y)$ can then be readily obtained from $\langle \vec{e}_t, \vec{h}_t \rangle$ as

$$\Re(x,y)=\frac{\langle \vec{e}_t, \vec{h}_t \rangle}{\mathcal{F}(f)}. \tag{21}$$

By eliminating repeated computation of the double summation of the integrations, the computation of the strip-line to strip-line discontinuity or ridge waveguide to ridge waveguide discontinuity can be as fast as that of empty waveguide discontinuity problems, excluding the computation of the frequency-independent part of the inner product.

D. Modeling of Probe Coupling of the Comb-Line Resonators

The probe coupling structures shown in Fig. 1 can be rigorously solved by considering them as cascaded structures of a series of discontinuities. The cross-section of the comb-line resonator inner conductor can be rectangular or circular in shape. For the case of a rectangular inner conductor, the inner conductor section can be considered as a piece of ridge waveguide with empty waveguide discontinuities, as shown in Fig. 5(a). The cylindrical inner conductor resonator can be rigorously modeled using the modeling method described in [10] or approximated by stair steps using a series of ridge waveguide to ridge waveguide discontinuities. Fig. 5(b) shows the S-matrix network representation of the rectangular resonator inner conductor, where $[S^{R,E}]$ and $[S^{E,R}]$ are generalized scattering matrices of ridge and empty waveguide discontinuities. L represents the length of the rectangular rod. Applying the generalized S-matrix cascading procedure [7], [8], the generalized scattering matrices of the whole resonator rod $[S^{\text{reso}}]$ can be obtained.

The shape of the coupling probe can be a straight rectangular bar or have an additional larger cross-section piece at both ends of the probe, in between the comb-line resonators and through the common resonator wall of the two cavities. The cylindrical shaped coupling bar can be approximated by the square cross-section bar with same area. The half-probe coupling structure is treated as a cascaded structure of an empty waveguide to strip-line and strip-line to strip-line discontinuities. An additional piece of strip-line and its discontinuity are added for the modeling of the dumbbell shape coupling probes shown in Fig. 6(a). The S-matrix network representation of the coupling probe is given in Fig. 6(b). Similar to the modeling procedure of the resonator rod, the generalized scattering matrices of the half-coupling probe $[S^{\text{probe}}]$ can be obtained.

With generalized S-matrices of the resonator rod and coupling probe, the probe coupling structure can then be accurately modeled. Fig. 7 shows the network representation of the coupling structures shown in Fig. 1. By cascading the generalized scattering matrices of all the discontinuities of the half-coupling structure, and applying PEC and PMC boundary conditions, the coupling coefficient of the probe coupling can be accurately determined from the resonant frequencies f_e and f_m obtained from applying the terminating conditions at the symmetrical plane [10].

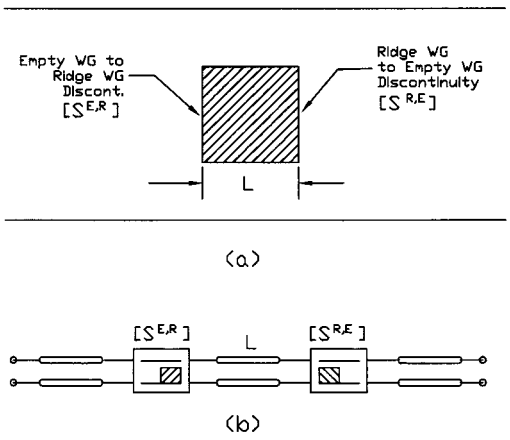

Fig. 5. Top view and network representation of a rectangular comb-line resonator rod.

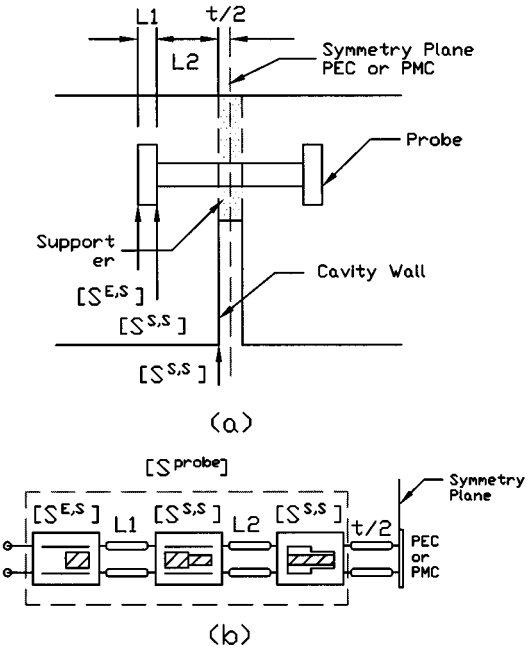

Fig. 6. Side view and network representation of a coupling probe with larger diameter ends through the cavity wall.

III. Numerical Results

Computer programs have been developed to compute the electric probe couplings between comb-line resonators with either rectangular or cylindrical resonator inner conductor. Convergence tests on the numerical results were first performed by analyzing the eigenmode's parameters of the strip-line. Fig. 8 shows the convergence of the dominant mode's characteristic impedance and the cutoff wave number k_c^2 of the first

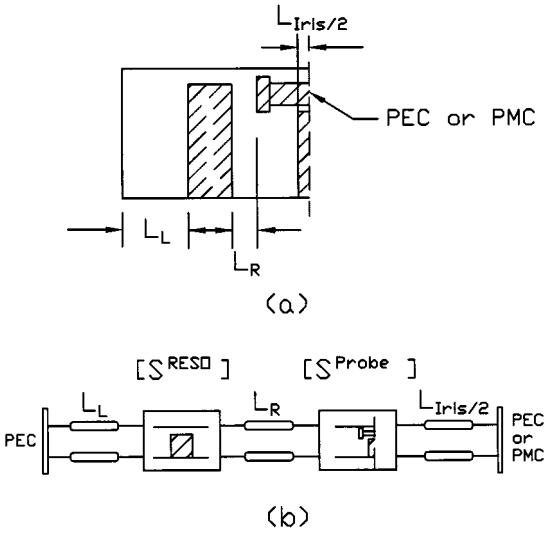

Fig. 7. Network representation of the coupling structure.

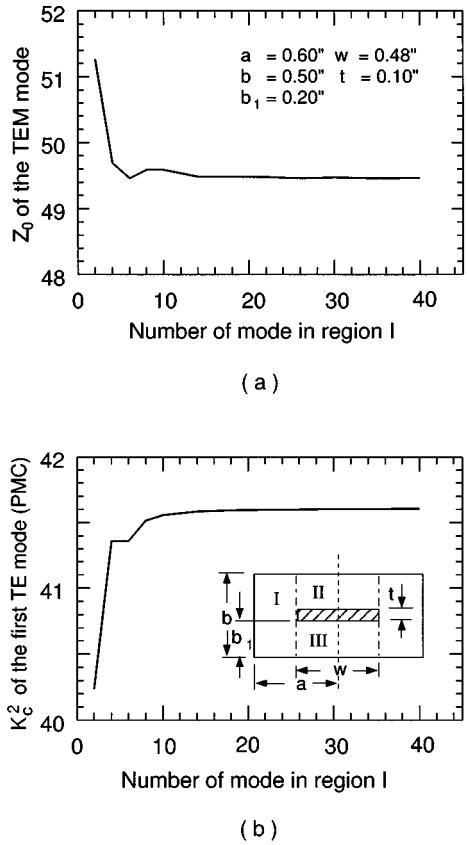

Fig. 8. The convergence of the results. (a) Convergence of the characteristic impedance of the TEM mode. (b) Convergence of the cutoff wave number of the first TE mode.

high-order mode in the shielded strip-line with $a = 0.60''$, $b = 0.50''$, $b_1 = 0.20''$, $w = 0.48''$, and $t = 0.10''$ versus the number of eigenmodes used in region I, while the number of eigenmodes used in region II and III is taken by ratio. It is shown that convergent results can be obtained when the number of basis functions in region I is greater than 16.

Fig. 9 shows the normalized cutoff frequency versus $w/2a$ for different TE modes in the shielded strip-line of zero thickness t

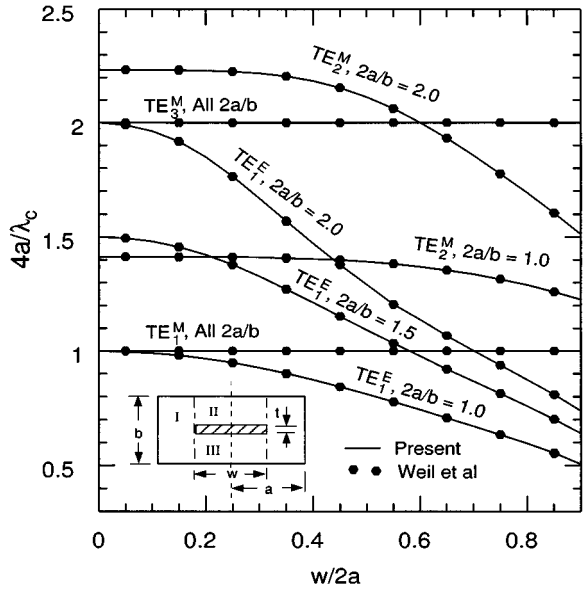

Fig. 9. Normalized cutoff frequency versus $w/2a$ for different TE modes in shielded strip-lines.

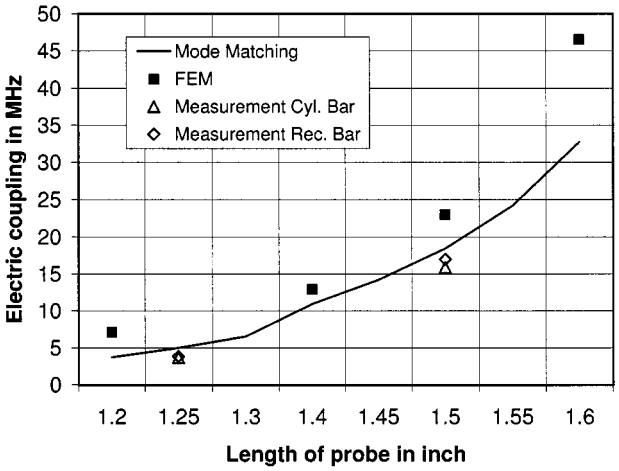

Fig. 10. Computed electric probe (0.25×0.25 in^2) coupling between two comb-line resonators with $0.50 \times 0.50 \times 1.40$ in^3 (H) rectangular inner conductors in a $2.0 \times 2.0 \times 1.50$ in^3 (H) enclosure versus the length of the probe bar in the center of 0.50×0.50 in^2 aperture.

and compared with the results by Weil *et al.* [5]. The numerical results by two methods are in excellent agreement. It is observed that the TE_1^M mode cutoff remains unaltered by the presence of the zero-thickness strip conductor and continues to be governed by the criterion $\lambda_c = 4a$. Furthermore, the characteristics for TE_1^E mode cutoff cross the TE_1^M mode cutoff characteristics for all values of $2a/b > 1.0$. For $2a/b \leq 1.0$, the TE_1^E mode cutoffs are below those of the TE_1^M mode.

Fig. 10 presents the computed electric probe coupling between two comb-line resonators with rectangular inner conductors versus the length of the probe. Fig. 11 shows the computed coupling values of the probe between two resonators with cylindrical inner conductors. It is seen that the electric coupling increases at a faster rate as the probe moves closer to the inner conductor of the resonator. The computed results are compared

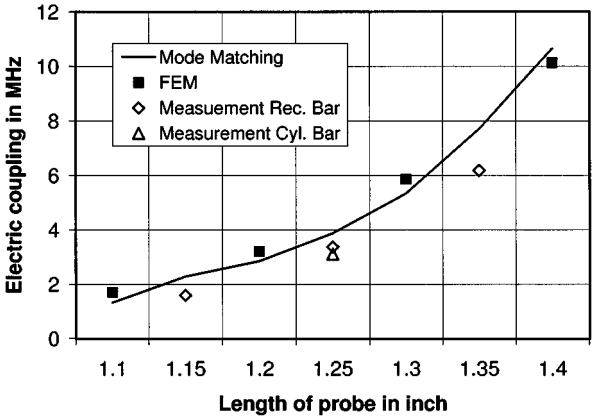

Fig. 11. Computed electric probe (0.25×0.25 in^2) coupling between two comb-line resonators with 0.50-in DIA $\times$ 1.40-in (H) cylindrical inner conductors in a $2.0 \times 2.0 \times 1.50$ in^3 (H) enclosure versus the length of the probe bar in the center of 0.50×0.50 in^2 aperture.

with that computed by finite-element method and from measurement and are shown to be in good agreement. The measured results also show that an electric probe with a square or cylindrical cross-section of same area can achieve almost the same coupling value because two probes have almost the same capacitance between the resonator inner conductor and the probe. Therefore, a cylindrical probe can be approximated by a rectangular one with the same area.

IV. Conclusions

The electric coupling probes of the comb-line resonators were rigorously modeled by full-wave mode matching method. The probe coupling structures were solved by cascading the generalized scattering matrices of the resonator's inner conductor and probe discontinuities. The electric probe couplings between comb-line resonators with both rectangular and cylindrical inner conductor can be obtained by computing the resonant frequencies of the coupling structure. The accuracy of the method was verified by comparing the numerical results with the measured data and finite-element method and was shown to be in good agreement.

References

[1] G. L. Matthaei, "Comb-line band-pass filters of narrow or moderate bandwidth," *Microwave J.*, vol. 6, pp. 82–91, Aug. 1963.

[2] R. Levy and J. D. Rhodes, "A comb-line elliptic filter," *IEEE Trans. Microwave Theory Tech.*, vol. MTT-19, pp. 26–29, Jan. 1971.

[3] A. E. Atia and A. E. Williams, "Narrow bandpass waveguide filters," *IEEE Trans. Microwave Theory Tech.*, vol. MTT-20, pp. 258–265, Apr. 1972.

[4] G. L. Matthaei, L. Young, and E. M. T. Jones, *Microwave Filters, Impedance-Matching Networks and Coupling Structure*. New York: McGraw-Hill, 1984.

[5] C. M. Weil, W. T. Joins, and J. B. Kinn, "Frequency range of large-scale TEM mode rectangular striplines," *Microwave J.*, vol. 24, pp. 93–97, Nov. 1981.

[6] R. R. Mansour, R. S. K. Tong, and R. H. Macphie, "Simplified description of the field distribution in finlines and ridge waveguides and its application to the analysis of E-plane discontinuities," *IEEE Trans. on Microwave Theory and Techniques*, vol. 36, pp. 1825–1832, Dec. 1988.

[7] R. Mittra and J. R. Pace, "A new technique for solving a class of boundary value problems," *IEEE Trans. Antennas Propagat.*, vol. AP-11, p. 617, Sept. 1963.

[8] A. S. Omar and K. Schönemann, "Transmission matrix representation of finline discontinuities," *IEEE Trans. Microwave Theory Tech.*, vol. MTT-33, pp. 765–770, Sept. 1985.

[9] H. W. Yao, A. Abdelmonem, J.-F. Liang, X.-P. Liang, K. A. Zaki, and A. Martin, "Wide band waveguide and ridge waveguide T-junctions for diplexer applications," *IEEE Trans. Microwave Theory Tech.*, vol. 41, pp. 2166–2173, Dec. 1993.

[10] H. W. Yao, K. A. Zaki, A. E. Atia, and R. Hershtig, "Full wave modeling of conducting posts in rectangular waveguides and its applications to slot coupled combline filters," *IEEE Trans. Microwave Theory Tech.*, vol. 43, pp. 2824–2830, Dec. 1995.

[11] C. Wang and K. A. Zaki, "Full-wave modeling of generalized double ridge waveguide T-junctions," *IEEE Trans. Microwave Theory Tech.*, vol. 44, pp. 2536–2542, Dec. 1996.

Chi Wang (SM'98) received the B.S. and M.S. degrees from Beijing Institute of Technology, Beijing, China, in 1983 and 1986, respectively, and the Ph.D. degree from the University of Maryland, College Park, in 1997, all in electrical engineering.

From 1986 to 1989, he was an Electrical Engineer with the North China Vehicle Research Institute, Beijing. From 1990 to 1992, he was with Beijing New Asia Electronics Inc. He spent one year as a Research Associate at the Beijing Institute of Technology working on modeling of antennas and resonators using the finite difference time-domain method. From 1994 to 1997, he held a Graduate Research Assistantship with Microwave Research Group, University of Maryland at College Park, where he worked on analysis, modeling, and design of microwave circuits and devices. He was a Graduate Teaching Assistant between 1994 and 1995. In 1997, he joined Radio Frequency Systems Inc., where he held several technical positions and is now Engineering Manager. He has authored or coauthored more than 40 technical papers in the area of numerical methods and modeling of resonators and filters. His current research interests include new microwave resonator and filter technology, numerical technology, and computer-aided design of advanced RF and microwave circuit for wireless communication systems.

Kawthar A. Zaki (SM'85–F'91) received the B.S. degree (with honors) from Ain Shams University, Cairo, Egypt in 1962 and the M.S. and Ph.D. degrees from the University of California, Berkeley, in 1966 and 1969, respectively, all in electrical engineering.

From 1962 to 1964, she was a Lecturer in the Department of Electrical Engineering, Ain Shams University. From 1965 to 1969, she was a Research Assistant in the Electronics Research Laboratory, University of California, Berkeley. She joined the Electrical Engineering Department, University of Maryland, College Park, in 1970, where she is presently a Professor of electrical engineering. Her research interests are in the areas of electromagnetics, microwave circuits, simulation, optimization, and computer-aided design of advanced microwave and millimeter-wave systems and devices. She has more than 200 publications and five patents on filters and dielectric resonators.

Prof. Zaki has received several academic honors and awards for teaching, research, and inventions.